Intellectual Journal of Energy Harvesting and Storage
Vol. 3, No. 2, December 2025, pp. 86~97
ISSN: 2963-6272, DOI: 10.11591/ehs.v3i2.pp86-97

Co-integrated energy-harvesting and radio frequency transmission structure for Ku-band applications

Ikram Troudi[1], Chokri Baccouch[2], Rhaimi Belgacem Chibani[1]
[1]MACS Laboratory: Modeling, Analysis, and Control of Systems LR16ES22, National Engineering School of Gabes, University of Gabes, Medenine, Tunisia
[2]LR-Sys'Com-ENIT, Communications Systems LR-99-ES21 National, Engineering School of Tunis, University of Tunis, Tunis, Tunisia

Article Info

Article history:

Received Aug 4, 2025
Revised Nov 19, 2025
Accepted Dec 14, 2025

Keywords:

Energy harvesting
Internet of things
Ku-band
Meshed patch
Photovoltaic antenna
Radio frequency/direct current decoupling

ABSTRACT

This paper presents the design, optimization, and simulation of a compact meshed antenna integrated with a photovoltaic (PV) cell for simultaneous Ku-band wireless communication and solar energy harvesting. The proposed structure leverages the front metallic grid of the solar cell as both a radiating patch and an energy-collecting surface, enabling compact, and autonomous radio frequency (RF) operation. A comprehensive mathematical model was developed to minimize key loss mechanisms—including series resistance, contact resistance, metal resistivity, and optical shadowing—associated with the grid geometry. The optimization process identified an optimal finger width of 28 µm that maximized energy conversion efficiency while maintaining high-quality RF radiation. The antenna is implemented on a multilayer silicon substrate and operates at a resonant frequency of 16.55 GHz with a simulated −10 dB bandwidth of 390 MHz. A peak gain of 4.24 dBi and a directivity of 8.67 dB were achieved. An RF/direct current (DC) decoupling circuit was also integrated to ensure functional independence between the energy harvesting and communication subsystems, with negligible impact on return loss. This dual-function system offers a promising solution for the development of compact, energy-autonomous wireless platforms, particularly suited for internet of things (IoT) applications, smart infrastructure, and remote sensing in space-constrained environments.

Corresponding Author:

Chokri Baccouch
LR-Sys'Com-ENIT, Communications Systems LR-99-ES21 National, Engineering School of Tunis
University of Tunis
1002, Tunis, Tunisia
Email: chokri.baccouch13@gmail.com

1. INTRODUCTION

Since the 1970s, microstrip antennas-commonly referred to as patch antennas-have witnessed significant advancement, propelled by breakthroughs in microelectronics, particularly in miniaturization, and multilayer circuit integration. The rapid evolution of wireless communication systems has intensified the need for compact, energy-efficient, and easily integrable antennas capable of maintaining high RF performance across various embedded and portable platforms [1], [2].

Simultaneously, the widespread deployment of autonomous systems-such as wireless sensors, internet of things (IoT) devices, and remote monitoring units-has underscored the necessity for reliable and sustainable power sources. Energy autonomy has become a key requirement for next-generation wireless nodes, especially in remote or infrastructure-limited environments. Photovoltaic (PV) cells have therefore

emerged as a natural solution, offering renewable and maintenance-free energy harvesting capabilities. However, integrating PV cells with radio frequency (RF) components within a confined form factor introduces several technical challenges, including mutual electromagnetic interference, increased optical and ohmic losses, and stringent geometric constraints [3]-[5].

Recent research efforts have consequently shifted toward multifunctional hybrid structures that combine solar energy harvesting and electromagnetic radiation within a single compact architecture. Such co-integrated systems aim not only to reduce physical volume and system cost, but also to improve overall energy efficiency and enable long-term autonomous operation. A critical factor governing the performance of these architectures is the design of the front metal grid, which must simultaneously act as a PV energy collector and a radiating RF element without compromising either function [6], [7].

In this context, the present work proposes the design and simulation of a meshed patch antenna co-integrated with a PV cell using a shared radiating aperture, specifically tailored for Ku-band wireless communication. The Ku-band (12–18 GHz), widely employed in satellite communications, backhaul links, and high-data-rate point-to-point systems, is gaining increasing relevance in the context of 5G and beyond. Despite this growing importance, most existing PV antenna designs remain limited to lower frequency bands, such as C-band or 2.4 GHz. Targeting a higher frequency operation at 16.55 GHz, this work demonstrates the feasibility of compact, efficient, and energy-autonomous RF nodes in the Ku-band.

The primary objective of this study is to develop a dual-function structure capable of achieving efficient solar energy conversion while preserving reliable RF transmission performance. To this end, a comprehensive analytical model is employed to quantify and minimize the optical and electrical losses associated with the front metal grid. The optimization process explicitly addresses the trade-off between optical shadowing, ohmic losses, and RF radiation efficiency, which constitutes a fundamental challenge in PV antenna co-design.

The resulting structure is implemented on a multilayer silicon substrate to ensure electromagnetic compatibility and stable dielectric behavior at high frequencies. An RF/direct current (DC) decoupling network is also integrated to guarantee functional isolation between the energy harvesting path and the RF signal path, thereby preventing performance degradation due to mutual coupling. The proposed antenna achieves a peak gain of 4.24 dBi, a directivity of 8.67 dB, and a−10 dB impedance bandwidth of 390 MHz centered at 16.55 GHz.

The novelty of this work lies in the reuse and mathematical optimization of the PV front metal grid as a shared radiating aperture for Ku-band transmission, enabling simultaneous energy harvesting and RF communication without additional radiating elements or structural redundancy. This approach provides a compact and energy-aware solution suitable for IoT gateways, smart infrastructure, and autonomous wireless platforms operating in space-constrained environments.

The remainder of this article is structured as follows: section 2 reviews recent related work and highlights the motivation for this study. Section 3 details the proposed antenna architecture and optimization method. Section 4 presents and discusses the simulation results. Finally, section 5 concludes the paper and outlines future research directions.

2. RELATED WORKS AND MOTIVATION

The rapid evolution of telecommunication systems, combined with the growing demand for self-powered devices, has accelerated the development of hybrid solutions that integrate radiating antennas with energy-harvesting units. Energy autonomy has become a central design constraint for modern wireless systems, particularly for IoT nodes, remote sensors, and smart infrastructure deployed in isolated or hard-to-access environments. Among the various approaches investigated, the integration of microstrip patch antennas with PV cells has emerged as a promising strategy to simultaneously address challenges related to device compactness, energy autonomy, and electromagnetic performance. Such co-integrated structures support both RF signal transmission and solar energy collection, aligning with the objectives of green communication systems aimed at reducing dependence on conventional power sources and batteries.

Recent studies have demonstrated the feasibility and advantages of multifunctional PV antenna architectures. Xue *et al*. [8], a reconfigurable reflect array composed of a 14×14 grid of solar cells integrated with PIN diodes was proposed to enable 1-bit beam-steering functionality with two phase states (0°/180°). Operating at 2.4 GHz, the array achieved a peak gain of 16.6 dBi and an impedance bandwidth of 28.3%, while simultaneously harvesting solar energy to power the reconfiguration circuitry. This work highlights the potential of combining energy harvesting and beamforming capabilities within a single structure, paving the way toward adaptive and self-powered wireless systems.

Beyond reconfigurability, optical transparency has emerged as a critical requirement for antennas intended to be co-integrated with solar panels or deployed on transparent surfaces such as building windows or vehicle windshields. Emon *et al*. [9], an optically transparent microstrip patch antenna was developed

using a soda-lime glass substrate and indium tin oxide (ITO) for both the radiating patch and the ground plane. Designed for 5G C-band applications, the antenna achieved a gain of 1.247 dB at 5.3 GHz and exhibited a wide bandwidth of 990 MHz due to ground plane modifications. This configuration demonstrates that transparent conductive materials can enable concurrent RF operation and solar energy harvesting, making them suitable for smart and energy-autonomous systems.

Further innovations have explored spatial adaptability through three-dimensional antenna geometries. Arboleda *et al*. [10], a transparent microstrip patch antenna system was integrated into a dodecahedron-shaped acrylic structure hosting twelve individually controlled antennas. The proposed system achieved 96% optical transparency and a gain of 6.1 dBi at 2.45 GHz. The directional reconfigurability enabled by RF switching allowed the antenna to steer its radiation toward a desired base station, thereby reducing power wastage and improving energy efficiency. This work underlines the relevance of pattern diversity and meshed conductor structures in advanced RF/PV co-integration scenarios.

Beyond compactness and energy efficiency, intelligent antennas capable of mitigating electromagnetic pollution have attracted increasing interest, particularly in IoT sensing applications. Arboleda and Shamim [11], a self-powered and cost-effective air quality monitoring node was presented, employing an optically transparent and reconfigurable meshed antenna embedded within a compact dodecahedral housing. With a peak gain of up to 14.8 dB in selected directions and an optical transparency of 87%, the system enabled targeted wireless transmission while reducing the overall footprint by nearly 80% compared to conventional planar arrays. Field experiments demonstrated the system's ability to detect localized air pollution events that conventional weather stations failed to identify, validating the effectiveness of combining solar energy harvesting with intelligent antenna architectures for real-world sensing applications.

Emerging research has also investigated advanced materials for high-frequency energy-harvesting antennas. John *et al*. [12], a solar-powered rectangular patch antenna based on graphene was designed to operate at 0.57 THz for wireless sensor network applications. The antenna exhibited a gain of 6.81 dBi, a return loss of −51 dB, and a radiation efficiency of 55%, while harvesting solar energy to charge a storage element. Although limited to simulation results, this work demonstrates the feasibility of ultra-high-frequency PV antennas for future compact and autonomous wireless platforms.

In light of these contributions, it is evident that the functional integration of energy-harvesting and radiating structures represents a strategic enabler for the development of compact, energy-aware, and autonomous wireless systems. However, the vast majority of reported designs operate in low-to-mid frequency bands, such as 2.4 GHz or C-band, where physical dimensions are relatively large and coupling effects are less critical. Very few studies have addressed higher-frequency bands such as the Ku-band (12–18 GHz), where tighter electromagnetic constraints, increased losses, and fabrication sensitivity pose significant challenges. Moreover, there remains a lack of comprehensive investigations focused on the joint optimization of the PV front metal grid for both minimal energy loss and efficient RF radiation, particularly at Ku-band frequencies.

In this work, we propose the design and optimization of a meshed antenna structure co-integrated with a PV cell and dedicated to Ku-band wireless communication at 16.55 GHz. The originality of the proposed approach lies in reusing the solar cell's front metal grid as a shared radiating aperture, enabling simultaneous solar energy harvesting and RF transmission without additional radiating elements. A rigorous mathematical model is developed to minimize total electrical, optical, and resistive losses associated with the grid geometry. Using this model, optimal geometrical parameters are derived to maximize collected solar power while preserving high RF performance. The resulting antenna structure is simulated using Multiphysics electromagnetic tools, and its key characteristics—including reflection coefficient (S11), radiation pattern, gain, and directivity—are thoroughly analyzed. This work contributes to the development of compact, energy-autonomous RF modules suitable for embedded sensors, intelligent nodes, and wireless communication platforms operating in constrained or isolated environments. Table 1 (see Appendix) [8]-[12] summarizes and compares representative related works.

3. DESIGN AND MODELING

In this section, we present the design of a co-integrated PV antenna system that simultaneously fulfills the requirements of solar energy harvesting and RF transmission in the Ku-band. As illustrated in Figure 1, the proposed architecture converts incident solar radiation into electrical power to supply all active electronic components of the wireless node. The same physical structure is used for both energy harvesting and RF radiation through a shared aperture configuration, where the PV front metal grid also acts as a meshed radiating patch. Any excess harvested energy is directed toward a storage element to ensure continuous system operation during periods of low or no solar exposure. This co-design approach enables

end-to-end energy autonomy, from solar energy collection to RF transmission, while avoiding the use of separate antennas or external power sources.

In conventional wireless systems, depicted in Figure 2, the antenna and the power source are implemented as separate and independent units. Electrical power is typically supplied by batteries, which inherently limit the operational lifetime and require periodic maintenance or replacement. The antenna is either embedded within the device enclosure or externally mounted to ensure RF communication. Such architectures increase system volume, weight, and complexity, while also introducing additional interconnections and potential sources of loss. In contrast, the integrated PV antenna proposed in this work provides a compact, multifunctional solution that combines energy harvesting and RF transmission within a single structure, thereby reducing system size, weight, and cost, while improving long-term reliability and sustainability.

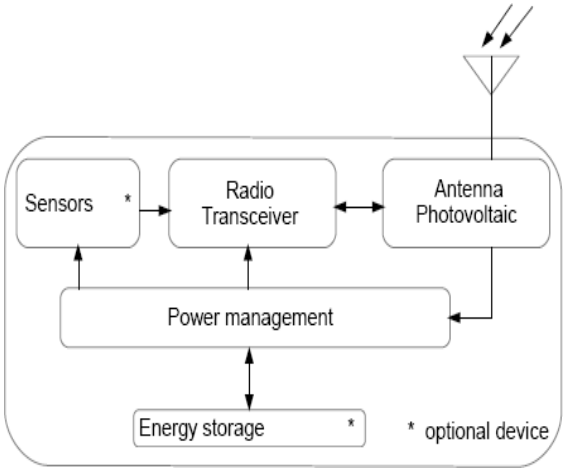

Figure 1. Autonomous wireless system using the PV antenna

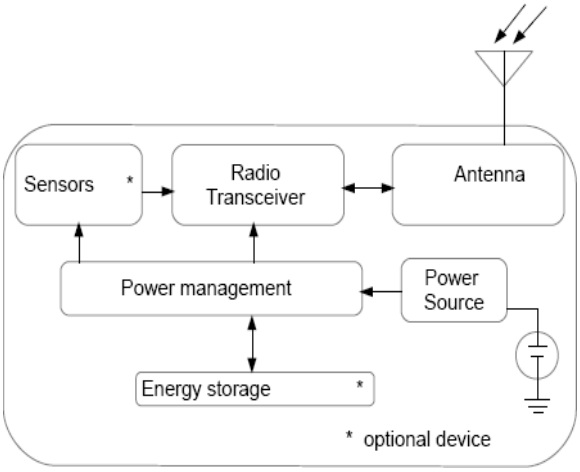

Figure 2. Conventional wireless system block diagram

The proposed antenna is specifically designed to simultaneously satisfy two critical and often conflicting functionalities: high-efficiency solar energy harvesting and reliable RF transmission in the Ku-band (12–18 GHz). The structure builds upon the concept of reusing the front metal grid of a PV cell as a meshed patch antenna, which significantly optimizes space utilization and minimizes structural redundancy. This shared-aperture co-integration strategy allows RF radiation and PV collection to coexist without introducing additional radiating layers or separate antenna elements. Such a dual-purpose configuration is particularly advantageous for wireless systems requiring compactness, low power consumption, and maintenance-free operation in remote, outdoor, or space-constrained environments.

3.1. Structural composition

The proposed antenna is implemented on a multilayer silicon-based architecture, as illustrated in Figure 3, specifically optimized for Ku-band operation at 16.55 GHz. The topmost layer consists of a meshed metallic grid, which plays a dual role: it collects incident photons for PV energy conversion and simultaneously serves as the RF radiating patch. The geometry of this grid is carefully designed to balance optical transparency, electrical conductivity, and RF radiation efficiency.

Beneath the metallic mesh, an n-type silicon layer with a thickness of 0.5 μm and a relative permittivity of ε_r=11.9 is employed to facilitate charge separation. This layer is followed by a p-type silicon layer with a thickness of 300 μm and ε_r=11.8, forming the active PV junction responsible for electrical energy generation. The entire structure is electrically isolated from the ground plane by a SiO_2 dielectric layer with a thickness of 1.5 mm and ε_r=3.9. This dielectric spacer ensures electromagnetic isolation, reduces substrate losses, and provides stable dielectric behavior at high frequencies.

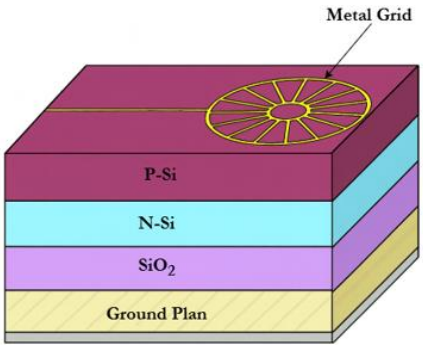

Figure 3. Antenna layer structure

This multilayer configuration enables the co-integration of RF and PV functionalities within a single compact structure, while ensuring electromagnetic compatibility and stable operation in the Ku-band. The choice of silicon-based materials and dielectric stacking is particularly suitable for high-frequency operation, where substrate losses, dispersion, and coupling effects become critical. The proposed architecture thus forms a robust foundation for the joint optimization of energy harvesting efficiency and RF radiation performance at 16.55 GHz.

3.2. Optimization of the metal grid geometry

A major challenge in achieving the desired dual functionality lies in the optimization of the PV front metal grid, illustrated in Figure 4, which has a direct and coupled impact on both optical transparency and electrical conductivity, and consequently on the overall PV and RF performance of the structure. At Ku-band frequencies, the grid geometry additionally influences current distribution, surface losses, and radiation efficiency, making its optimization a critical design step.

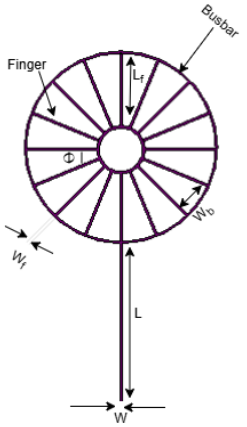

Figure 4. Collection grid front face of a PV cell

To improve the energy conversion efficiency of the PV cell while preserving adequate RF radiation characteristics, the geometrical parameters of the metal grid were optimized by minimizing the combined effect of four dominant loss mechanisms directly associated with the front metal mesh. These losses are mathematically expressed by in (1)-(4) [13]-[20] and are defined as:

- Series resistance power loss: resulting from the resistance along the fingers of the metallic grid due to their finite conductivity and length.

$$P_1 = \frac{\rho_s J_{mp} L_f^2 \theta}{6V_{mp}} \quad (1)$$

- Front contact resistance loss: arising from the interface between the front contact and the semiconductor material, particularly relevant in high-frequency operation.

$$P_2 = \frac{\rho_m J_{mp} L_f^3 \theta}{5 V_{mp} W_f} \quad (2)$$

- Metal resistance loss: caused by resistive heating within the grid itself due to current flow.

$$P_3 = \frac{\rho_c J_{mp} L_f \theta}{V_{mp} W_f} \quad (3)$$

- Optical shadowing loss: due to the partial obstruction of incident solar radiation by the metallic grid, which reduces the effective photoactive surface area.

$$P_4 = \frac{L_f W_f}{L_f W_f + L_f^2 \theta} \quad (4)$$

The total dissipated power is given by the sum:

$$P_T = \sum_{i=1}^{4} P_i$$

Figure 4 illustrates the PV collection grid, which simultaneously acts as the radiating surface of the antenna, thereby highlighting the inherent coupling between PV and RF functionalities. Other loss mechanisms commonly encountered in solar cells, such as recombination losses or shunt resistance, are assumed to be independent of the grid geometry and are therefore excluded from the present optimization analysis [15], [16]. The useful power collected by the PV cell is defined as:

$$P_{col} = P_{in} - P_T$$

where:
P_{in}: incident solar power
P_T: total power dissipated due to resistive and optical losses

This expression constitutes the basis of the optimization strategy, which aims to maximize the collected power while maintaining acceptable RF radiation performance. The optimization is carried out by adjusting key grid parameters such as finger width, spacing, and orientation angle θ. This trade-off-driven approach ensures a balanced compromise between PV efficiency and RF radiation efficiency, which is essential for shared-aperture co-integrated systems. The optimized grid is subsequently employed in the antenna structure simulated and analyzed in the following sections.

3.3. Geometrical and electrical parameters

The key geometrical parameters of the optimized solar cell antenna are summarized in Table 2. Among these parameters, the width of the metallic fingers was identified as the most sensitive variable, as it directly governs the balance between optical and electrical losses. Narrow fingers reduce optical shadowing but increase series resistance, whereas wider fingers reduce resistive losses at the expense of increased optical obstruction. An optimal trade-off value was therefore determined through combined analytical modeling and numerical simulations.

Table 2. Dimensions of the solar cell antenna

Symbol	Values	Description
θ	20°	Angle
L_f	3.5 mm	Length of fingers
L	7.11 mm	Length of inset feed
W_b	0.5 mm	Width of bus bars
W_f	28 µm	Width of fingers
W	0.233 mm	Width of inset feed

To accurately model the PV losses associated with the optimized grid, the physical and electrical parameters listed in Table 3 were employed. These parameters describe the material properties of the silicon layers, metal contacts, and grid composition, and were selected based on realistic PV fabrication constraints.

Table 3. Parameters used for PV cell loss modeling

Symbol	Values	Description
θ	22.5°	Angle
Jm	0.03 A.cm^{-2}	Areal density of current
ρ_s	40 Ω.cm	Resistance of layer of the transmitter
ρ_c	5.10^{-5} Ω.cm	Resistivity of contact front face
ρ_m	1.10^{-5} Ω.cm	Resistivity of metal
T	7.5 µm	Thickness of metal
V_m	0.5 V	Voltage of the cell

These sets of geometrical and electrical parameters were incorporated into a multiphysics simulation environment, enabling a quantitative evaluation of the combined impact of grid geometry on both PV energy conversion efficiency and RF radiation performance. This unified modeling framework is essential to accurately capture the trade-offs inherent to shared-aperture RF/PV co-integration at Ku-band frequencies.

4. SIMULATION RESULTS AND DISCUSSIONS

The performance of the proposed PV antenna was evaluated through a comprehensive simulation-based analysis carried out in two sequential stages. The first stage focused on the optimization of the front metal grid to maximize PV energy harvesting efficiency, while the second stage investigated the RF behavior of the co-integrated antenna, including impedance matching, radiation characteristics, and the effectiveness of the RF/DC decoupling strategy. This two-step evaluation allows a clear separation between PV optimization and RF performance assessment, while highlighting their mutual interaction within a shared-aperture architecture.

4.1. Optimization of the finger width

One of the most critical parameters influencing the PV performance of the proposed structure is the width of the metallic fingers forming the front grid. Narrow fingers reduce optical shadowing and increase light absorption but lead to higher series resistance, whereas wider fingers improve electrical conductivity at the expense of increased optical obstruction. This antagonistic behavior establishes a clear trade-off between optical and electrical losses, which must be carefully optimized to maximize the harvested power.

Figure 5 illustrates the variation of the collected PV power as a function of the finger width. The curve exhibits a pronounced maximum, corresponding to the optimal compromise between reduced resistive losses and limited optical shadowing.

As observed, the collected power initially increases with finger width due to the reduction of resistive losses along the metallic grid. Beyond a certain threshold, however, further increasing the finger width leads to a degradation of performance caused by excessive optical shadowing. The optimal finger width was identified as 28 µm, which was subsequently adopted in all RF simulations. This value represents a balanced solution that preserves PV efficiency while ensuring adequate current distribution for high-frequency RF operation.

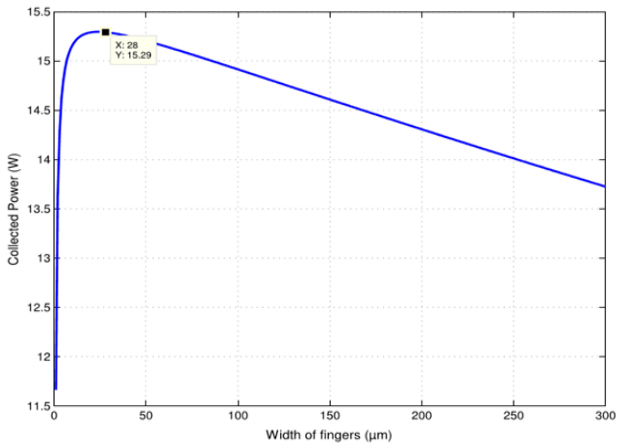

Figure 5. Collected power according to width of fingers

4.2. Loss modeling and cell parameters

To accurately model the PV behavior of the proposed antenna, a multicrystalline silicon substrate was considered. The electrical parameters of the front surface, including contact resistivity and metal thickness, are summarized in Table 2, while the rear surface was assumed to be fully metalized with aluminum. This assumption ensures good electrical continuity and enhances the reflective properties of unabsorbed photons, thereby improving overall PV efficiency.

This comprehensive modeling approach enables a realistic estimation of the harvested energy under standard illumination conditions and provides reliable input parameters for the subsequent RF simulations. By incorporating both material and geometrical characteristics, the model captures the coupled influence of PV and electromagnetic phenomena.

4.3. Antenna structure and return loss

Following the optimization of the front grid, the complete antenna structure was implemented on the multilayer silicon substrate composed of n-type silicon, p-type silicon, and a SiO_2 dielectric layer, as described in the previous section. The antenna's impedance matching performance was evaluated by simulating the reflection coefficient S_{11}. Figure 6 shows the simulated S11 response of the antenna.

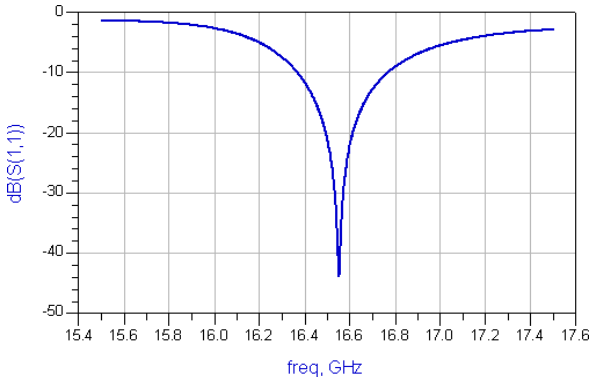

Figure 6. Reflection parameter S11

The antenna exhibits a clear resonance at 16.55 GHz, with a −10 dB impedance bandwidth of approximately 390 MHz. The return loss at resonance is lower than −20 dB, indicating excellent impedance matching and minimal reflected power. These results confirm that the integration of the PV grid does not compromise the antenna's matching characteristics, validating the suitability of the proposed design for Ku-band wireless communication systems.

4.4. Radiation characteristics

The radiation behavior of the proposed antenna was evaluated at its resonant frequency of 16.55 GHz. The two-dimensional far-field radiation patterns are shown in Figure 7. The radiation pattern reveals a single dominant main lobe, indicating directional radiation characteristics that are well suited for point-to-point and backhaul communication scenarios. The antenna achieves a peak gain of 4.24 dBi and a directivity of 8.67 dB. These values demonstrate that the meshed PV grid, despite its dual functionality, does not significantly degrade the radiation performance, confirming the effectiveness of the shared-aperture design for RF transmission applications.

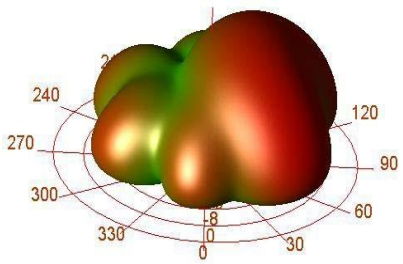

Figure 7. Radiation pattern of the antenna

4.5. RF/DC decoupling circuit design

To ensure the simultaneous and interference-free operation of the energy harvesting and RF transmission functions, an RF/DC decoupling circuit was designed and integrated into the system. This circuit enables the DC power extracted from the PV cell to be routed independently of the RF signal path, thereby preventing undesired coupling effects [21], [22]. The schematic of the decoupling circuit is depicted in Figure 8.

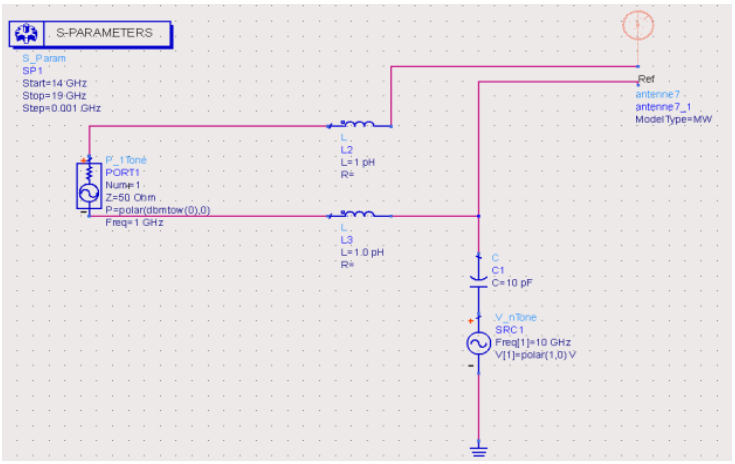

Figure 8. Solar cell antenna decoupling RF/DC circuit

The decoupling circuit incorporates passive filtering elements that provide high isolation between the RF port and the DC harvesting path. This configuration ensures stable operation of both subsystems without introducing additional RF losses or distortion. To further validate the effectiveness of the decoupling strategy, the equivalent circuit response was simulated, with particular attention given to the reflection coefficient after integrating the RF/DC network. The resulting response is presented in Figure 9. The reflection response remains consistent with the original S_11 characteristic shown in Figure 6, confirming that the RF/DC decoupling circuit does not introduce significant impedance mismatch or performance degradation in the RF path.

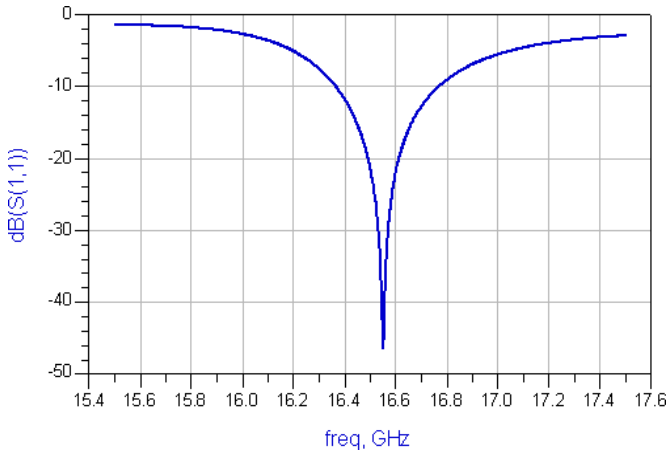

Figure 9. Simulation of equivalent circuit

4.6. Functional implications

The co-integration of the PV cell and antenna into a single compact structure offers substantial advantages over conventional wireless architectures, as illustrated earlier in Figure 2. Traditional systems

rely on separate components for energy harvesting and RF transmission, resulting in increased volume, cost, and system complexity. By unifying both functionalities within a shared physical structure, the proposed design significantly reduces system size, enhances energy autonomy, and improves deployment flexibility. Such characteristics make the proposed PV antenna particularly suitable for space-constrained and energy-limited applications, including smart city infrastructures, vehicular communication platforms, and autonomous IoT gateways operating in remote or outdoor environments.

5. CONCLUSION

This work presented the design and simulation of a compact meshed antenna co-integrated with a PV cell for simultaneous Ku-band wireless communication and solar energy harvesting. The originality of the proposed structure resides in the reuse and optimization of the PV cell's front metallic grid as a shared radiating aperture, enabling a dual-function system that combines energy autonomy and high-frequency RF transmission within a single physical layer, without introducing additional antenna elements or structural redundancy.

A rigorous mathematical optimization model was developed to minimize the dominant loss mechanisms associated with the grid geometry, namely series resistance, front contact resistance, metal resistivity, and optical shadowing losses. The optimization process identified an optimal finger width of 28µm, which represents an effective trade-off between electrical conductivity and optical transparency. This optimized configuration enhanced PV energy conversion while preserving the integrity of RF radiation performance, confirming the suitability of the shared-aperture approach.

The proposed antenna, implemented on a multilayer silicon-based substrate, demonstrated robust RF characteristics, including a resonant frequency of 16.55 GHz, a −10 dB impedance bandwidth of 390 MHz, a peak gain of 4.24 dBi, and a directivity of 8.67 dB. Furthermore, the integration of an RF/DC decoupling network ensured functional independence between the energy harvesting and RF transmission paths, with no observable degradation in impedance matching, thereby validating the effectiveness of the co-integration strategy.

Overall, the proposed hybrid PV antenna provides a compact, energy-autonomous, and high-frequency-capable solution well suited for next-generation wireless platforms. Its ability to operate efficiently in the Ku-band while maintaining PV functionality makes it particularly attractive for embedded IoT nodes, smart infrastructure, vehicular platforms, and remote sensing applications, where size, power availability, and maintenance constraints are critical.

Despite the promising simulation results, the present study is limited to numerical modeling and simulation-based validation. Future work will therefore focus on the fabrication and experimental characterization of the proposed structure, including over-the-air measurements, isolation analysis, and efficiency assessment under realistic illumination and RF excitation conditions. Further extensions will investigate reconfigurable, multiband, and optically transparent implementations, as well as the integration of energy storage and power management circuits, to enable fully autonomous and scalable deployments of PV antenna systems.

ACKNOWLEDGMENTS

This work was supported by LR- Sys'Com-ENIT, Communications Systems LR-99-ES21 National Engineering School of Tunis, University of Tunis.

FUNDING INFORMATION

Authors state no funding involved.

AUTHOR CONTRIBUTIONS STATEMENT

This journal uses the Contributor Roles Taxonomy (CRediT) to recognize individual author contributions, reduce authorship disputes, and facilitate collaboration.

Name of Author	C	M	So	Va	Fo	I	R	D	O	E	Vi	Su	P	Fu
Ikram Troudi	✓	✓	✓	✓	✓	✓		✓	✓	✓				
Chokri Baccouch		✓	✓	✓	✓	✓	✓	✓		✓	✓	✓	✓	
Rhaimi Belgacem				✓			✓			✓	✓		✓	✓
Chibani														

C : **C**onceptualization
M : **M**ethodology
So : **So**ftware
Va : **Va**lidation
Fo : **Fo**rmal analysis
I : **I**nvestigation
R : **R**esources
D : **D**ata Curation
O : Writing - **O**riginal Draft
E : Writing - Review & **E**diting
Vi : **Vi**sualization
Su : **Su**pervision
P : **P**roject administration
Fu : **Fu**nding acquisition

CONFLICT OF INTEREST STATEMENT

The authors declare no conflict of interest.

DATA AVAILABILITY

The data used during the current study are available from the corresponding author on reasonable request.

REFERENCES

[1] M. K. Titaouine, "Analysis of Antennas Micro Ruban by the Model of the Cavity, the Model of the Transmission Line and the Method of Moments," University Ferhat Abbas, Setif, 1998.
[2] A. Taflove and M. E. Brodwin, "Numerical Solution of Steady-State Electromagnetic Scattering Problems Using the Time-Dependent Maxwell's Equations," *IEEE Trans. Microw. Theory Tech.*, vol. 23, no. 8, pp. 623–630, 1975, doi: 10.1109/TMTT.1975.1128640.
[3] S. V. Shynu, M. J. R. Ons, P. McEvoy, M. J. Ammann, S. J. McCormack, and B. Norton, "Integration of Microstrip Patch Antenna With Polycrystalline Silicon Solar Cell," *IEEE Trans. Antennas Propag.*, vol. 57, no. 12, pp. 3969–3972, Dec. 2009, doi: 10.1109/TAP.2009.2026438.
[4] T. W. Turpin and R. Baktur, "Meshed patch antennas integrated on solar cells," *IEEE Antennas Wirel. Propag. Lett.*, vol. 8, pp. 693–696, 2009, doi: 10.1109/LAWP.2009.2025522.
[5] M. Danesh and J. R. Long, "An autonomous wireless sensor node incorporating a solar cell antenna for energy harvesting," *IEEE Trans. Microw. Theory Tech.*, vol. 59, no. 12 PART 2, pp. 3546–3555, 2011, doi: 10.1109/TMTT.2011.2171043.
[6] T. Bendib and F. Djeffal, "Electrical performance optimization of nanoscale double-gate MOSFETs using multiobjective genetic algorithms," *IEEE Trans. Electron Devices*, vol. 58, no. 11, pp. 3743–3750, 2011, doi: 10.1109/TED.2011.2163820.
[7] A. Taflove, S. C. Hagness, and M. P-May, "Computational Electrodynamics, the Finite-Difference Time-Domain Method," *Electr. Eng. Handb.*, vol. 3, no. 15, pp. 629–670, 2005.
[8] F. Xue *et al.*, "A Self-Powered Electronically Reconfigurable Reflectarray Integrated with Solar Cells," *IEEE Antennas Wirel. Propag. Lett.*, vol. 23, no. 11, pp. 3441–3445, 2024, doi: 10.1109/LAWP.2024.3440338.
[9] E. I. Emon, A. M. Islam, M. S. Bashar, and A. Ahmed, "Performance Evaluation of an Optically Transparent Microstrip Patch Antenna for 5G Applications Using ITO and Sodalime Glass Substrate," *Comput. Electr. Eng.*, vol. 114, p. 109073, 2024, doi: 10.2139/ssrn.4592413.
[10] M. B. Arboleda, M. Vaseem, and A. Shamim, "Optically Transparent Microstrip Patch-Based Antenna with 3D Pattern Diversity," *17th Eur. Conf. Antennas Propagation, EuCAP*, 2023, doi: 10.23919/EuCAP57121.2023.10133360.
[11] M. B. Arboleda and A. Shamim, "Self-Powered and Cost-Effective Wireless Sensor Node for Air Quality Monitoring With an Optically Transparent Smart Antenna System," *IEEE Sens. J.*, vol. 24, no. 18, pp. 28457–28471, 2024, doi: 10.1109/JSEN.2024.3435885.
[12] A. S. John, U. Gopalakrishnan, T. Joseph, and A. B Siraj, "Solar Powered Terahertz Antennas for Wireless Sensor Network Applications," *Int. Conf. Microwave, Antenna Commun. MAC 2023*, 2023, doi: 10.1109/MAC58191.2023.10177101.
[13] F. Djeffal, N. Lakhdar, and A. Yousfi, "An optimized design of 10-nm-scale dual-material surrounded gate MOSFETs for digital circuit applications," *Phys. E Low-Dimensional Syst. Nanostructures*, vol. 44, no. 1, pp. 339–344, 2011, doi: 10.1016/j.physe.2011.09.007.
[14] W. Liu, Y. Li, J. Chen, Y. Chen, X. Wang, and F. Yang, "Optimization of grid design for solar cells," *J. Semicond.*, vol. 31, no. 1, 2010, doi: 10.1088/1674-4926/31/1/014006.
[15] A. Cheknane, B. Benyoucef, J. P. Charles, R. Zerdoum, and M. Trari, "Minimization of the effect of the collecting grid in a solar cell based silicon," *Sol. Energy Mater. Sol. Cells*, vol. 87, no. 1–4, pp. 557–565, 2005, doi: 10.1016/j.solmat.2004.07.038.
[16] C. Bendel, J. Kirchhof, and N. Henze, "Application of photovoltaic solar cells in planar antenna structures," *Proc. 3rd World Conf. Photovolt. Energy Convers.*, vol. A, pp. 220–223, 2003, doi: 10.1049/cp:20030180.
[17] C. Baccouch, H. Sakli, D. Bouchouicha, and T. Aguili, "Patch antenna based on a photovoltaic solar cell grid collection," 2016 *Progress in Electromagnetic Research Symposium (PIERS)*, pp. 164–165, 2016, doi: 10.1109/piers.2016.7734278.
[18] G. Clasen and R. Langley, "Meshed Patch Antennas," *IEEE Trans. Antennas Propag.*, vol. 52, no. 6, pp. 1412–1416, Jun. 2004, doi: 10.1109/TAP.2004.830251.
[19] T. W. Turpin *et al.*, "Meshed Patch Antennas Integrated on Solar Cell - A Feasibility Study and Optimization," M.S. thesis, Dept. of Electrical Eng., Utah State University, Utah, United States, 2009.
[20] C. Baccouch, D. Bouchouicha, H. Sakli, and T. Aguili, "Optimization of the Collecting Grid Front Side of a Photovoltaic Cell Dedicated to the RF Transmission," *Proc. Eng. Technol.*, vol. 2, pp. 72–77, 2015.
[21] P. Morvillo, E. Bobeico, F. Formisano, and F. Roca, "Influence of metal grid patterns on the performance of silicon solar cells at different illumination levels," *Mater. Sci. Eng. B*, vol. 159–160, no. C, pp. 318–321, 2009, doi: 10.1016/j.mseb.2008.10.004.
[22] C. Baccouch, C. Bahhar, H. Sakli, N. Sakli, and T. Aguili, "Design of a Compact Meshed Antenna for 5G Communication Systems," *Int. J. Electron. Commun. Eng.*, vol. 13, no. 12, pp. 721–725, 2019.

APPENDIX

Table 1. Comparative table of energy-harvesting antenna technologies

Ref	Proposed structure	Freq (GHz)	Gain (dBi)	Optical transparency	Main functionality	Technology/materi	Originality
[8]	14×14 reconfigurable reflect array with solar cells and PIN diodes	2.4	16.6	Not specified	1-bit beam steering (0°/180°) + self-powering	Solar cells + PIN diodes	Integration of energy harvesting and beamforming
[9]	Optically transparent microstrip patch antenna	5.3	1.24	Yes	Communication + integration on glass surface	Soda-lime glass + ITO	Transparent antenna co-integrated with solar harvesting
[10]	3D transparent dodecahedral antenna system	2.45	6.1	96%	Spatially reconfigurable radiation pattern	Acrylic + meshed conductors	3D reconfigurability with optical transparency
[11]	Transparent meshed antenna in environmental sensor node	Not clearly specified	Up to 14.8	87%	Self-powered air quality monitoring with directional transmission	Compact dodecahedral structure + solar harvesting	80% size reduction + targeted wireless transmission
[12]	Graphene-based solar-powered patch antenna (simulated)	0.57 THz	6.81	Not specified	Terahertz wireless communication + battery charging	Graphene	High-frequency design with novel material
Our work	Meshed antenna integrated with photovoltaic front grid	16.55 (Ku-band)	4.24	Implied (via meshed structure)	Simultaneous RF transmission and solar energy harvesting	PV front grid reused as radiating patch	Mathematical optimization of grid for dual RF-PV function

BIOGRAPHIES OF AUTHORS

Ikram Troudi was born in Gafsa Tunisia, in 1995. A Ph.D. student in Genie Engineering at the National School of Engineering of Gabes (ENIG). She received a research master's degree in electronics and telecommunications from the Higher Institute of Computer Science and Multimedia of Gabes (ISIMG), Tunisia, in 2020. She received a Fundamental license in science and technology of information and communication from the Higher Institute of Applied Sciences and Technology of Gafsa (ISSAT Gaf), Tunisia, in 2017. She can be contacted at email: ikram.troudi@isimg.tn.

Chokri Baccouch was born in Gabes Tunisia, in 1988. Assistant Professor at Paris 8 University. He received Ph.D. in Telecommunications from the National School of Engineering of Tunis (ENIT), Tunisia in 2018. He received the National diploma in engineering Telecommunications and Networks from the National School of Engineering of Gabes (ENIG), Tunisia, in 2012. Our research works in IoT, artificial intelligence, communications systems, and harvesting energy. He can be contacted at email: chokri.baccouch13@gmail.com.

Rhaimi Belgacem Chibani is an Associate Professor in CSIE (Computer Sciences and Information Engineering). He joined the National Engineering High School at Gabes named (ENIG) where he is actually employed since September 1991. After a Doctorate Thesis earned at the National Engineering High School at Tunis (ENIT), he received the Ph.D. degree from ENIG, University of Gabes, Tunisia in 1992. He is a member of the Research Laboratory MACS at ENIG as activities supervisor dealing with signal processing and communications research field. Currently, his research areas cover signal processing and mobile communications. He can be contacted at email: abouahmed17@gmail.com.